Bull. Mater. Sci., Vol. 38, No. 2, April 2015, pp. 531–536. © Indian Academy of Sciences.

Effect of cooling rate on the microstructure and mechanical properties of a C–Mn–Cr–B steel

SMRITI OJHA[1,*], N S MISHRA[1] and B K JHA[2]
[1]National Institute of Foundry and Forge Technology, Ranchi 834 003, India
[2]Research & Development Centre for Iron and Steel, Steel Authority of India Limited, Ranchi 834 002, India

MS received 11 June 2014; revised 2 September 2014

Abstract. **The microstructure and mechanical properties of a low carbon steel containing 30 ppm boron have been investigated. The steel was subjected to various cooling conditions in a thermo-mechanical simulator to generate continuous cooling transformation (CCT) diagram. Similar cooling conditions were also applied to tensile samples in order to evaluate their mechanical properties. The results indicate profuse banding in the hot strip of thickness 2.5 mm. This effect is attributed to the presence of manganese. In addition, variation in cooling rate led to increase in strength but severely affected percentage elongation albeit in an acceptable limit of 6%. This effect is discussed in the light of degree of banding of strips and microstructural constituents generated during heat treatment of steel strips of different thicknesses.**

Keywords. **Boron; ultra-high strength steel; thermo-mechanical simulation; CCT diagram; banded structure.**

1. Introduction

Low carbon steels having manganese content between 1.0 and 1.5 wt% have been found suitable for applications in automotive industries in view of their improved formability. To increase strength, boron is added in the ppm range. Phase transformation attributes of the steel is exploited to improve strength upon cooling after deformation. The development of steel for this particular application is still in nascent stage and their studies are confined to few laboratories across the globe. Hence, the car bodies will require steels with ultra-high strength. The constraint that accompanies this attribute is loss of ductility and consequent deterioration in formability. Hot stamping process was developed and patented by a Swedish company[1] and over the last thirty-five years has been found to be the most suitable process for fabrication of automotive parts. It is evident from the foregoing that hot stamping has caught up the fascination of metallurgists and process engineers for practical applications in shaping industrial products particularly automotive components. Many authors have reviewed the work in this area over the past two decades.[1–4] The research work of Akerstrom[5] and Naderi[6] are of relevance to the present investigation. At ambient temperature the steel blank has predominantly ferrite–pearlite structure. When the blank is heated above Ac3 temperature in austenite field and the forming is carried out by transferring it to tooling die when the steel still has austenitic structure then, the subsequent quenching at the cooling rate between 50 and 100°C s^{-1} has resulted in martensitic structure to attain strength of upto 1600 MPa.[6] Although, this is accompanied by decrease in ductility but it has little significance in post-deformation. Spring back forms recoverable part of elastic strain in the framework of total strain. This has severe effect on the geometrical stability of the formed component. As all the deformation is carried out in the austenite phase and at high temperature, wherein the reduced flow stress is encountered, the spring back phenomena can be minimized. The foregoing clearly envisages the search for appropriate grade of steel with right chemistry for enhanced strength and acceptable level of formability. The processing sequence and schedule need to be worked out carefully to achieve the above twin objectives. Boron alloying in steels induces good hardenability at low cooling rates.[7] The effect of boron addition in various grades of steels has been deftly summarized by Naderi.[6] The 22MnB5 boron alloyed steel is the common steel which has been traditionally used for hot stamping. This steel has acceptable hardenability and produces fully lath martensitic microstructure after hot stamping. With above consideration in mind the steel chosen for the present studies has principal constituents of 0.22C–1.26Mn–0.28Si–0.16Cr and 30 ppm boron. The final rolled product had a thickness of 2.5 mm. The composition of steel has been selected for the present study based on the rigorous literature review. The continuous cooling transformation (CCT) diagram of the above steel generated using a thermo-mechanical simulator is reported together with its microstructure and mechanical properties.

*Author for correspondence (smritiojha2008@gmail.com)

2. Experimental

2.1 *Material selection*

The steel samples were collected from Bokaro Steel Limited (BSL) of Steel Authority of India Limited (SAIL). Steel samples for chemical analysis was cut into the pieces of 35×35 mm^2 cross-section. The steel chemistry was ascertained by using optical emission spectroscope (OES) Model-THERMO, ARL 3460. The steel composition so obtained is given below: C – 0.22, Mn – 1.26, P – 0.015, S – 0.008, Si – 0.28, Al – 0.044, Ti – 0.023, Cr – 0.16, B – 30 ppm. The steel was made through continuous casting route and subsequently hot rolled to a thickness of 2.5 mm. The strip was further cold rolled down to various thicknesses as 0.8/1.0/1.2/1.6/1.8/2/2.5 mm. The samples for the present studies were however fabricated from the transfer bar of thickness 32 mm for phase transformation studies in the thermo-mechanical simulator as this requires samples of 10 mm diameter. The samples for heat treatment, on the other hand, were made from cold rolled sheets of various thicknesses as pointed out above.

2.2 *Thermo-mechanical simulation using Gleeble-3500*

Cylindrical samples with 85 mm length and 10 mm diameter were made from a 32 mm transfer bar for use in the dilatometer investigations in order to ascertain phase transformation characteristic. On the basis of the dilatometer plots for several cooling rates, CCT curves were drawn. The steel samples were first soaked at 900°C above the Ac_3 temperature in the simulator for 120 s, presuming that this will be adequate for chemical and structural homogenization. They were subsequently cooled to room temperature by employing cooling rates ranging from 0.2 to 36°C s^{-1}. The dimensional changes in these specimens during cooling were recorded using an ultra-sensitive dilatometer provided with the simulator and the output obtained as *dilatation plots*. Start and finish temperatures of transformed phases were identified from these plots.

2.3 *Heat treatment and mechanical testing*

Flat specimens were prepared with gauge length 55 mm and gauge width 10 mm for heat treatment in order to assess effect of thermal treatment on mechanical properties of the steel. The thermal treatment was carried out by heating the sample in the austenite single phase range at 900°C and holding it for 300 s followed by quenching in different media such as water, hot water, oil and air blow. The tensile test data were used for the measurement of elongation. The mechanical properties of steels were evaluated using an Instron-1195 universal testing machine. All tests were performed at room temperature. Rockwell hardness test was performed at room temperature to measure the macro-hardness of the specimens in B and C scales. The load was applied through the diamond indenter for few seconds during the testing of samples. Five measurements for each sample were carried out covering the whole surface of the specimen. The average was taken to get the final hardness result. A load of 100 and 150 kg, respectively, were applied for 30 s. The depth of indentation was automatically recorded on a digital gauge in arbitrary hardness number. These values were then converted to Brinell hardness number.

2.4 *Microstructural characterization*

Samples for microstructural observations were fabricated from the steels of 10×15 mm^2 cross-sectional dimensions. The samples were hot mounted using conducting resins and prepared for viewing in the microscope employing standard practices. To reveal the microstructure, the specimens were etched with 6% nital (6 ml nitric acid+94 ml methanol), albeit the nitric acid content is slightly higher than the usual. At lower acid concentration the images looked fuzzy. The samples were viewed in optical microscope Olympus model Gx71, whereas scanning electron microscope Zeiss model MEA10 was used for microstructural examination. All microstructural features including band width, grain size, interlamellar spacing, etc. were measured using quantitative metallography techniques following the linear intercept method described by Underwood.[8]

3. Results and discussion

3.1 *Microstructural studies*

Figure 1a shows the microstructure of hot rolled strip of 2.5 mm which consists of typical ferrite-pearlite phase mixture. The pearlite positioning has given the appearance of banding which is quite prominent. The microstructure continues to show strong evidence of banding in cold rolling upto a reduction of 28 pct. The banding, however started dissipating as the reduction during cold working is increased to 36 pct. Figure 1b shows the optical micrograph of the sample cooled at a slow cooling rate, i.e., 1°C s^{-1}. The micrograph reveals completely dominated by ferrite and pearlite phase mixture. However, in the case of latter coarse pearlite colony size is slightly larger. The formation of proeutectoid ferrite has occurred along the prior austenite grain boundary. Due to slow cooling the sample mainly constitutes the ferrite–pearlite mixture. Figure 1c gives first indication of the formation of bainite which can be perceived at cooling rate of 10°C s^{-1}. The bainite volume fraction has increased due to increase in the rate of cooling, i.e., 20°C s^{-1}, which can be discerned from figure 1d. In this case there is no sign of martensite revealed which is resolved with certainty only through transmission electron microscopy.

Figure 2 shows that the pearlite content in the microstructure has reduced and also as the reduction is increased the band width reduces consistently from 24 to 14 μm as the cold reduction is increased from 20 pct to a reduction of 68 pct. The variation is almost linear. The relation between

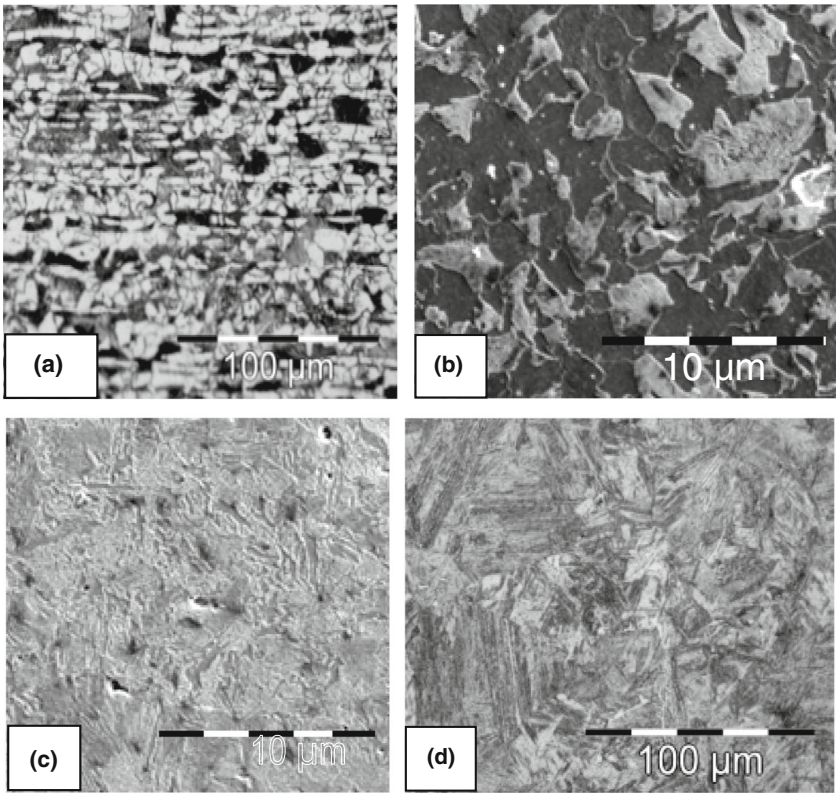

Figure 1. (**a**) Optical micrograph of banded structure of as-received sample, (**b**) SEM of ferrite–pearlite aggregate of the sample cooled at 1°C s^{-1}, (**c**) SEM of bainitic structure of the steel subjected to cooling rate of 10°C s^{-1} and (**d**) optical micrograph of martensitic structure at cooling rate of 20°C s^{-1}.

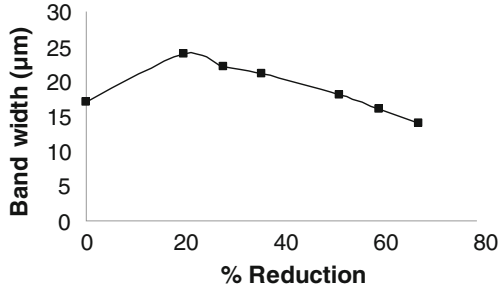

Figure 2. Variation in band width with percentage reduction during cold rolling.

bandwidth (BW) and per cent cold reduction (CR) has been worked out through regression analysis. A linear equation of type BW $= m$(CR) $+C$ expresses the correlation admirably. Here the slope, $m = -0.2009$ and the intercept on BW axis, $C = 28.0059$. This clearly reflects the synchronism between macro- and micro-reduction. Although the banding in low carbon steels has been reported by earlier investigators,[9,10] the present work provides a better insight into this effect in boron-containing steel.

The microscopic studies indicated that the ferrite grain size decreased with the increase in cooling rates as shown in figure 3a. However, further decrease in ferrite grain size is arrested and the curve levels off at ferrite grain size of ~5 µm. The plateau may indicate that if yet faster cooling rate is applied, the instability might occur in the phase structure and mark the commencement of another phase, perhaps bainite. Careful observation of the microstructures would reveal that there is remarkable disparity in volume fraction of ferrite associated with different cooling rates. It is interesting to note that at the fastest cooling rates of 20°C s^{-1}, the ferrite volume fraction has gone down significantly. This is reflected in the plot of figure 3b. Ferrite content, in the sample cooled at the rate of 0.2°C s^{-1}, has been determined to be ~80 pct, which has diminished to ~15 pct after cooling at a rate of 20°C s^{-1}. The variation is quite smooth, though a kink appears corresponding to cooling rates of 0.5 and 1.0°C s^{-1}. The interlamellar spacing decreases from 3.5 µm at the slowest cooling rate employed in the present studies to ~1.8 µm at the fastest cooling rate of 20°C s^{-1} as shown in figure 3c. It is standard practice to assess the efficacy of cooling by measuring hardness of the samples cooled at the different cooling rates. At slower cooling rates, upon transformation, clearly the ferrite phase dominate with some amount of pearlite. Ferrite being softer phase will impart lower hardness to steel. Further increase in hardness is due to decrease in pearlite interlamellar spacing as indicated from figure 3d. Continued enhancement in cooling rate will result in the change of shape of ferrite grains, which will become acicular or if

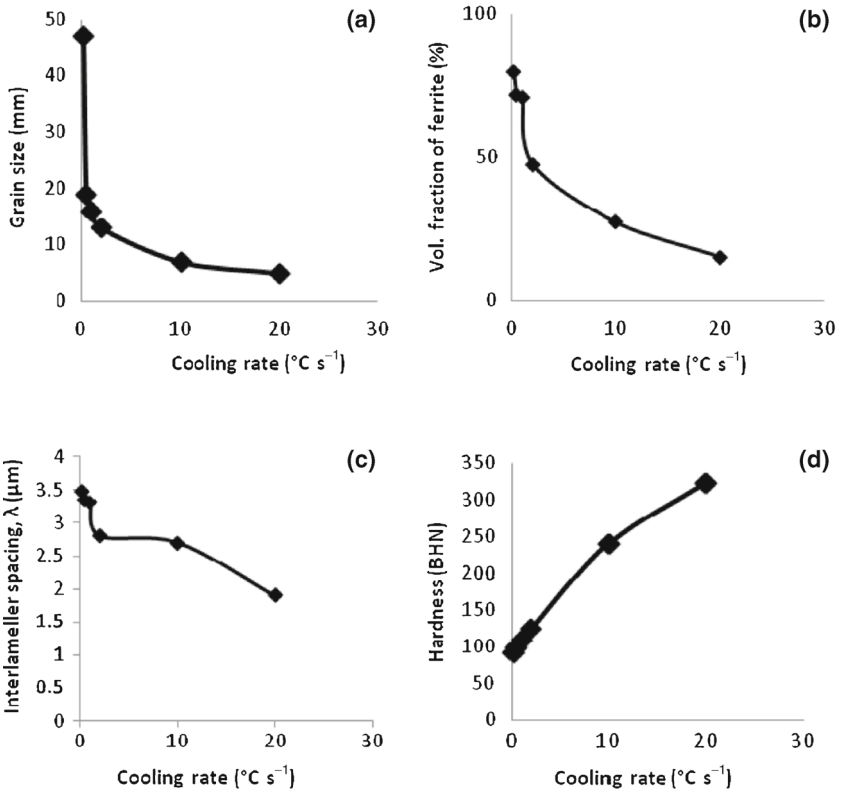

Figure 3. Effect of cooling rate on microstructural constituents and the resultant hardness variation.

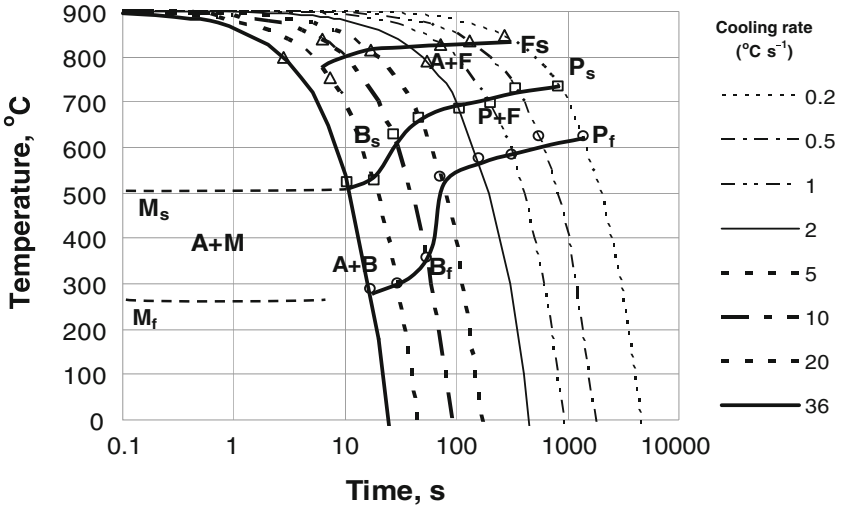

Figure 4. CCT diagram of C–Mn–Cr–B steel providing various phase fields in different cooling rate conditions.

the conditions are favourable will lead to formation of Widmanstten ferrite. In both the conditions will result in increase in hardness. At still higher rate of cooling much harder phase such as bainite and martensite are engendered. This will lead to rapid increase in hardness.

Phase transformation studies are crucial in determination of microstructure to be engendered in the materials. Dilatometer is one such method which finds wide applications in the investigation of transformation characteristics. It works on the principle of disparity in coefficients of thermal expansion (contraction) of different phases during heating (cooling) of the material. The change in phase will be reflected as change in slope of the temperature–dilation plot.

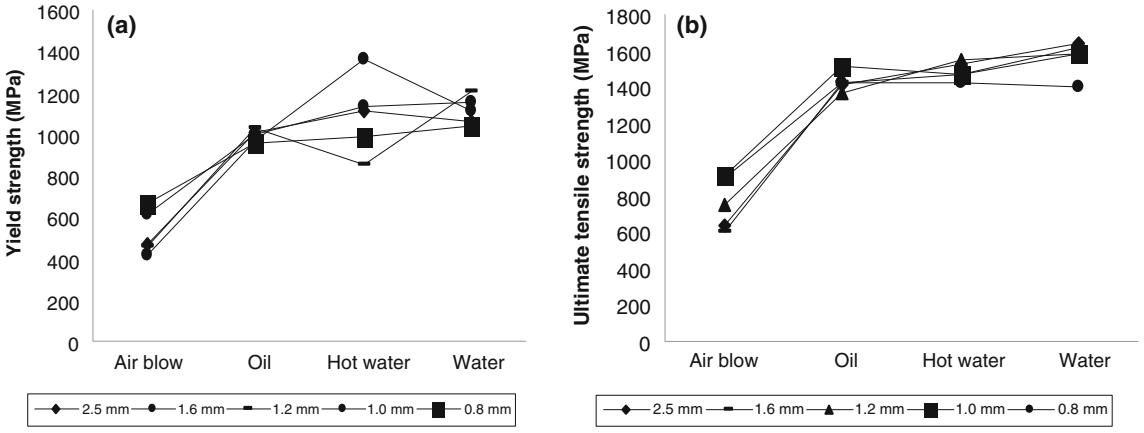

Figure 5. Variations in (**a**) YS and (**b**) UTS of the steel under different quenching conditions.

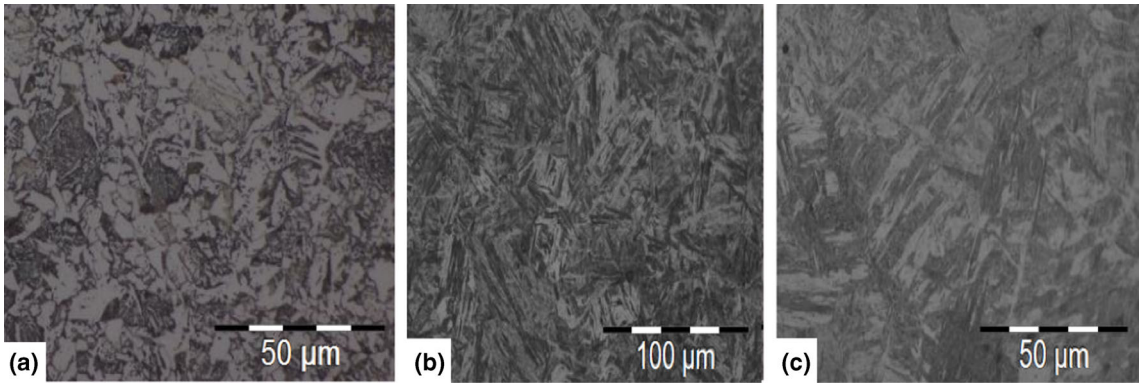

Figure 6. Optical micrograph of bulk heat treated samples (**a**) cold air blow, (**b**) oil quench and (**c**) cold water quenched.

It can be inferred from figure 4 that at all the curves associated with different transformation temperatures have diminishing tendencies as the cooling rate is increased. However, decrease is gradual upto cooling rate of 5°C s^{-1}. The proclivity towards decline becomes quite sharp at and above cooling rates of 10°C s^{-1}, which continues till it again levels off at cooling rates of 20°C s^{-1} and beyond. The CCT diagram can be interpreted in terms of first formation of proeutectoid ferrite from austenite labelled Ar_3 line. There is not much variations in this temperature with cooling rates. The region between Ar_3 line and the P_s line gets widened upon increase in cooling rates. The lines representing P_s and P_f remain somewhat parallel upto cooling rate of 5°C s^{-1}. Marked change in width of separation occurs after this cooling rate and area get widened progressively as it approaches towards higher cooling rates. Therefore, cooling rate of 5°C s^{-1} is critical and seems to be the signal departure from formation of mere pearlite and ferrite phase mixture. This may also be the cooling rate above which bainite may form. In summary, CCT diagram of boron modified steel clearly indicates the role of boron in influencing the microstructure of the steel. These behaviours have been reported to be as a result of B–N interaction in various forms.[11,12] Consequently, the steel should have complete lath martensite in the final structure for optimum property combination in order to meet the requirements for fabrication of car bodies by hot stamping.

3.2 *Mechanical properties*

In order to assess the effect of cooling rates on the final product after hot stamping, thermal treatments were imparted to the samples. The yield strength of samples of all the thicknesses increases with the increase in cooling rate and falls in the range of 400–650 MPa after cooling by cold air blow (CR ~ 25°C s^{-1}). Expectedly, the thinnest sample produced greatest enhancement in yield strength. However, surprisingly, when cooled in oil (CR ~ 36°C s^{-1}), despite rise in yield strength due to more rapid cooling, the incremental rise is somewhat oblivious to thickness. It can be noted that, for all thicknesses the yield strength values are approximately ~1.0 GPa. When the quenching is carried out in warm water at 75°C with estimated cooling rate of 90°C s^{-1}, the yield strength attains a value of ~1.4 GPa. The large variation in YS values is attributed to the varying proportions of microstructural constituents. The use of cold water raises the cooling rate to 180°C s^{-1}, and the range of yield strength is between 1.0 and 1.2 GPa as shown in figure 5a. Except for

thickness of 1.6 mm, the use of still water has little effect on yield strength. The variations in ultimate tensile strength (UTS) and hardness values on the similar pattern as described for yield strength variation with varying cooling rates using different cooling media for different thicknesses of samples. However maximum UTS of 1.6 GPa can be achieved with use of still cold water as cooling medium as shown in figure 5b. The cooling rate has been estimated to be 180°C s^{-1}. The microstructures of the heat treated samples provide a valuable insight into the variation in strength of the steel. The slow cooling rate arising from air cooling results in a ferrite–pearlite aggregate as shown in figure 6a in contrast to bainitic microstructure as shown in figure 6b of oil quench samples and the characteristic martensitic structure in water quenched steel presented in figure 6c. The microstructural features comprising ferrite–pearlite aggregate exhibit lower strength compared to the higher strength of steels having bainitic and martensitic structure of oil and water quenches steels.

4. Conclusions

The following conclusions are drawn from the aforementioned studies:

1. Occurrence of banding in the hot strip of thickness 2.5 mm has been linked to the presence of a relatively high manganese content as well as pancaking of austenite during subsequent deformation. In successive cold reductions the bandwidth is in synchronous with imposed amount of reduction. A linear relationship has been established between bandwidth (BW in μm) and cold reduction (CR in %) of the form; BW $= -0.2009 * (\mathrm{CR}) + 28.0059$.
2. The CCT diagram reflects various start and finish temperature of phase transformation corresponding to different cooling rates. It has been convincingly established that a threshold cooling rate of 20°C s^{-1} is essential to get acicular phase, i.e., bainite and or martensite.
3. It has been shown that ferrite grain size and its volume fraction decrease with the increase in cooling rates. Interlamellar spacing measurements of pearlite phase revealed the usual trend of decrease with the increase in cooling rate. In almost all the plots smooth curves have been obtained indicating amenability towards regression analysis. The above microstructural features influence the mechanical properties of the steel.
4. Strength of the steel increases with the increase in cooling rate of various quenching media which is found highest value of 1500 MPa in a water quenched samples due to the formation of martensitic structure.

Acknowledgements

We thank Research & Development Centre for Iron and Steel, Steel Authority of India Limited, Ranchi, for providing the laboratory facility and Dr. Anjana Deva, for valuable discussions, encouragement and support.

References

1. Karbasian H and Tekkaya A E 2010 *J. Mater. Process. Technol.* **210** 2103
2. Neugebauer R, Altan T, Geiger M, Kleiner M and Strezing A 2006 *Ann. CIRP* **55** 2
3. Hoffmann H, So H and Steinbeiss H 2007 *Ann. CIRP* **56** 1
4. Jesweit J, Geiger M, Engel U, Kleiner M, Schikorra M, Duflou J and Neugebauer R 2008 *CIRP J. Manuf. Sci. Technol.* **1** 2
5. Akerstrom P 2006 *Modelling and simulation of hot stamping*. Doctoral thesis (Lulea University of Technology)
6. Naderi M 2007 *Hot stamping of ultra-high strength steels*. MS thesis (Technischen Hochschule Aachen)
7. Deva A, Jha B K and Mishra N S 2011 *Mater. Sci. Eng.* **528** 7375
8. Underwood E E 1970 *Quantitative stereology* (Addison-Wesley Pub. Co.) pp. 40–70
9. Krauss G 2003 *Met. Mater. Trans. B* **34B** 781
10. Majka Ted F, Matlock D K and Krauss G 2002 *Met. Mater. Trans. A* **33A** 1627
11. Maitrepierre P, Thivellier D and Vernis J R 1977 *Microstructure and hardenability of low alloy boron containing steels, hardenability concepts with applications to steel* (Conference Proceeding, Chicago, 24–26 October 421)
12. Sharma R C and Purdy G R 1974 *Met. Trans.* **5** 939